Journal of Metallurgy and Materials Science, Vol. 63, No. 3-4, July-December 2021
Printed in India, © NML, ISSN 0972-4257

Conservation of Resources by Processing of Waste Dumped Iron Ore Fines

ABHISHEK KUMAR[1], AKULA SANKARA RAO[2] AND SHOBHANA DEY[1]*
[1]Mineral Processing Division, CSIR-National Metallurgical Laboratory, Jamshedpur, India
[2]Mineral Processing Division, P G Centre, Nandihalli, VSK University, Karnataka

Abstract : The dumped iron ore sample having 49.62% Fe, 6.96% SiO_2, 9.94% Al_2O_3, and 7.65% LOI was used for the present investigation. Characterization studies of the as-received sample reveal that major iron-bearing minerals present in the ore are hematite and goethite. The magnetite/ martitized magnetite is observed in minor traces. The major gangue minerals are clay and gibbsite followed by quartz.

The present study aims to enrich the iron values of dumped iron ore fines to produce a value-added product. The iron values present in the feed sample were enriched by removing silica and alumina. The deslimed feed was subjected to a Floatex Density Separator. A statistical factorial design matrix was followed for conducting the tests using the process variables as, teeter water flowrate, bed pressure, and pulp density. The underflow obtained from FDS content is 58.2% Fe and the product yield is 64.4%. For further enrichment of the Fe-grade of the U/F, it was ground to 150µm for better liberation. After desliming the ground product of U/F, Fe-grade could be improved to 60%, and further subjecting the deslimed product to magnetic separation enhances the Fe-grade to 62% with mass recovery of 44.5%. The final product produced from the dumped iron ore fines could be used for pellet feed.

Keywords: *Waste iron ore fines; Fine processing; Floatex density separator; Bed pressure; Desliming, Magnetic separation*

1. INTRODUCTION

Iron ore is the basic raw material used in the production of pig iron, sponge iron, and finished Steel. Steel being a core sector, it is integral to the growth of the economy and one of the measures for accessing development. Recently, iron ore demand has increased tremendously due to the rise in industrial applications and the global scenario for industrial development. The metallurgical requirements for iron concentrate conditions have increased, as far as the chemical composition and final concentrate stability are concerned, as the quality iron ore is not only required for stable blast furnace operation but also to enhance the efficiency of the blast furnace operation. Some of the critical issues related to iron ore which encompass the composition of the iron ore with low Fe and high Al-Si ratio, low strength, lower reducibility, low temperature softening and melting tendency needs to be addressed effectively. The exploitation of lean grade ores became necessary due to the depletion of the high-grade iron ores and the increased demands of the industry. Therefore, it becomes essential to beneficiate low-grade ores to make them amenable for blast furnace operation using appropriate mineral processing systems.

Iron ores in India are usually beneficiated simply by crushing, sizing, and washing in coarser sizes. Fines produced during crushing and grinding of the iron ores, in order to beneficiate them, are simply discarded because of low iron content, high silica, alumina content in their fine size. These fines thrown into the dumps are increasing over the years, creating a lot of environmental issues. Moreover, the increasing tonnage of these fines dumps calls for additional space to accommodate them for which a lot of land is required at or near the plant. It is imperative to utilize the low-grade ore or fines from dumps by suitable beneficiation technique to conserve the resource. It will also reduce the tonnage of waste.

The gravity separation technique is one of the economic processes, especially for iron ore fines where the density difference between the valuable and gangue minerals is more. This could be utilized for effective separation at the

Corresponding Author :
E-mail : sd@nmlindia.org

initial stage. The fines (< -1mm) could be processed by a Spiral concentrator or Floatex Density Separator (FDS). However, in a spiral concentrator, separation is affected by the combined effect of the centrifugal action with a multiple sluicing system where the surface water washes away the lighter grains, leaving the grains of heavy minerals concentrated in the deeper section of the trough. The Floatex density separator works on the principle of hinder settling. It has been used for the processing of manganese fines, chromite tailing, coal fines and other minerals [1-5]. It is an advanced hindered settling classifier, called a counter-current and autogenous teeter bed separator [6]. It makes use of differential settling rates of the particles to segregate them according to size, shape and density. It includes low cut points, previously unattainable efficiencies and short payback periods [7]. FDS can be used for the processing of the material size in the range of 800-75µm [8]. Thus, it is found to be effective for discarding the silica from the different minerals [9-10].

Keeping in view of the increasing demand of raw materials and depleting quality of the ore of the run-of mine (ROM), it is necessary to process the dumped fines. It is very important to utilize the waste as it significantly impacts mineral resources and environmental hazards. The present study highlights the interactive effects of the process variables of FDS on the processing of the dumped low-grade iron ore and its effective separation. In the investigation, an attempt has been made to process the dumped low-grade iron ore fines for its gainful utilization and to produce a value-added product for pellet making and resource conservation.

2. MATERIALS AND METHODS

2.1 Material

The raw material used for the present study was fine dumped iron ore sample of size of about 1mm and the origin is from the Eastern part of India. The sample was characterized by chemical analysis, size-wise chemical analysis, specific gravity, and mineralogical study. The chemistry of the sample studied determined by the wet conventional method is presented in Table 1. It was found that the silica and alumina content in the sample is quite high. The high LOI indicates the presence of hydrated minerals in the sample along with the silicate minerals.

Table 1: Chemical characterization of as received sample

Radical	Fe (T)	SiO_2	Al_2O_3	LOI
%	49.62	6.96	9.94	7.65

The distribution of particle size in the feed material was determined by analysing the 80% (d_{80}), 50% (d_{50}) passing sizes, and -74µm size fraction with their Fe-content and Fe distribution. The detailed mineralogical characteristic of the sample is described below.

2.1.1 Characterization

The mineralogical characterization of the as-received sample was carried out by using Orthoplan Microscope (Leica). Microscopic study reveals that hematite, goethite/ limonite and martitized magnetite are the iron-bearing minerals present in the sample. Among the iron-bearing minerals, hematite and goethite are present in major amounts, while magnetite/ martitized magnetite is noticed in very minor to traces. Hematite occurs as anhedral to subhedral-shaped grains and needle-shaped microcrystalline aggregates i.e specularite (Fig-1 A). Goethite occurs as colloform bands with alternating layers of hematite (Fig 1 C). Some of the places magnetite grains are partially or completely transformed to hematite and some unaltered remnants of magnetite are noticed within hematite grains. (Fig 1C). Clay and gibbsite are the dominant gangue minerals present in the sample followed by quartz. In places, clay is thoroughly intermixed/ intergrown with fine-grained hematite (Fig 1D). Globular inclusions of gangue minerals (gibbsite and quartz) are observed within the hematite grains (Figs. 1A &B).

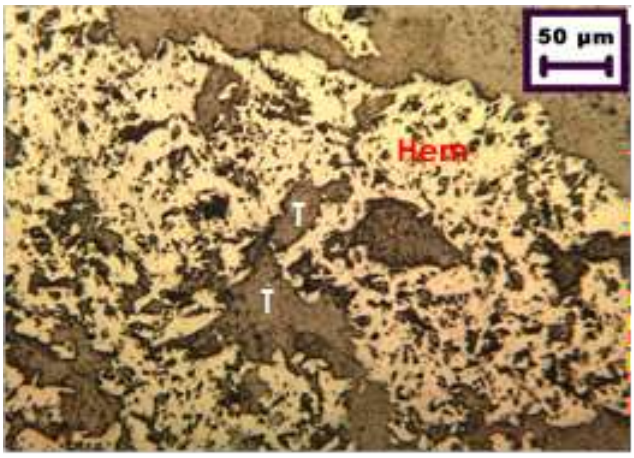

Fig 1A: hematite occurs as anhedral-shaped grains and is intricately associated with transparent gangues (clay, gibbsite & quartz).

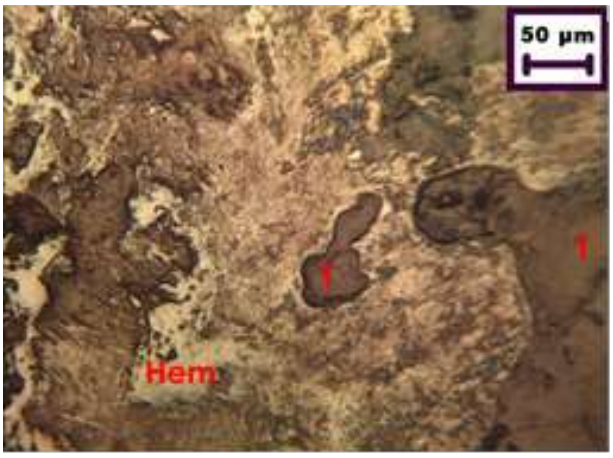

Fig. 1B: Hematite with transparent gangues (clay, gibbsite & quartz).

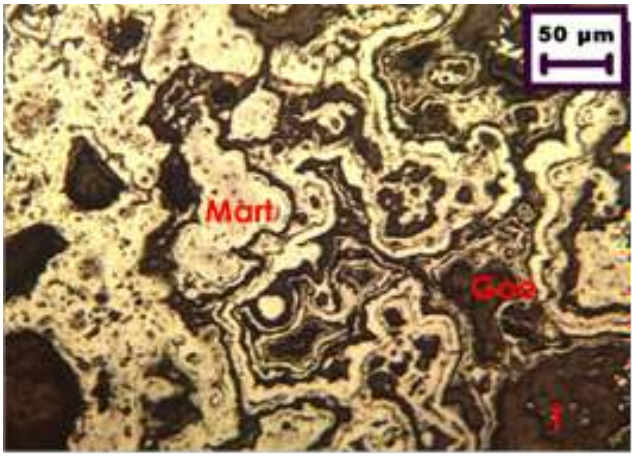

Fig 1C: Goethite occurs as colloform bands with alternating layers of hematite. Hematite replaces magnetite and remnants of unaltered magnetite found within hematite.

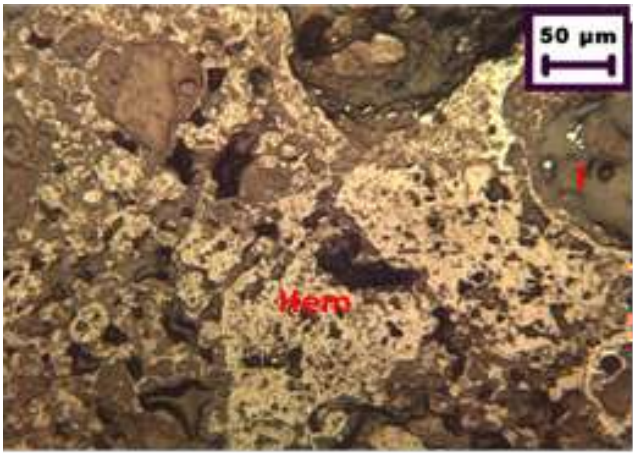

Fig 1D: Clay is thoroughly intermixed/ intergrown with fine-grained hematite.

Fig. 1: Photomicrographs showing the mineralogical characteristics and association of mineral phases present in the as-received sample. T- Transparent gangue (clay, gibbsite & quartz), Mart- Martitized magnetite, Hem-Hematite, Goe-Goethite.

2.2. Methods

The dumped iron ore fine sample was characterized with respect to the particle size distribution and each size fraction was analysed for Fe-content. Initial processing of the sample was carried out with Floatex Density Separator. In Floatex Density Separator (FDS), the three main zones as shown in Fig.2 are (i) upper zone (A) above the feed inlet (ii) intermediate zone (B) between the teeter water addition point and feed inlet, and (iii) lower section (C) below the teeter water addition point. Each zone plays a significant role in the separation of the feed based on their densities. Feed slurry is introduced to the FDS tangentially through a centralized feed well that extends to approximately one-third of the main tank length. Fluidizing (teeter water) is introduced over the entire cross-sectional area at the base of the teeter chamber through evenly spaced water distribution pipes. When the feed enters the main separation zone, it dilates into a fluidized bed by the rising current of water. The teeter water flow rate is dependent upon the particle size distribution in feed, density of the slurry, and the required cut-point for the separation. The separation takes place in zone B. The separated lighter/finer particles leave the separator

through zone A and the coarser/heavier particles through zone C. The FDS provides to maintain a constant height of the teeter bed and a steady discharge of the underflow [11]. The hindered settling involved in the separation prevails the effective separation compared to the spiral concentrator.

Floatex Density Separator works on the principle of fluidization and hindered settling in which the settling rate is affected by the neighbouring particles [12]. In hindered settling, the particles settle according to their size, shape, and specific gravity whereas, in free settling, the size and shape are the only factors that affect the particle settling velocity. The settling rate of particles in hindered settling environment could be determined by Newton's law. According to Newton's law, the settling rate presented in equation (1) indicates that the settling rate decreases with the increase of the pulp density. This is attributed to the increase in the particle-particle interference and thus, the viscosity of the medium.

$$v = \left[\frac{3gd(\rho_s - \rho_f)}{\rho_f}\right]^{1/2} \qquad \ldots. (1)$$

Where, v = settling rate of particle

d = diameter of particle, g = acceleration due to gravity

ρ_s = density of solid, ρ_f = density of fluid

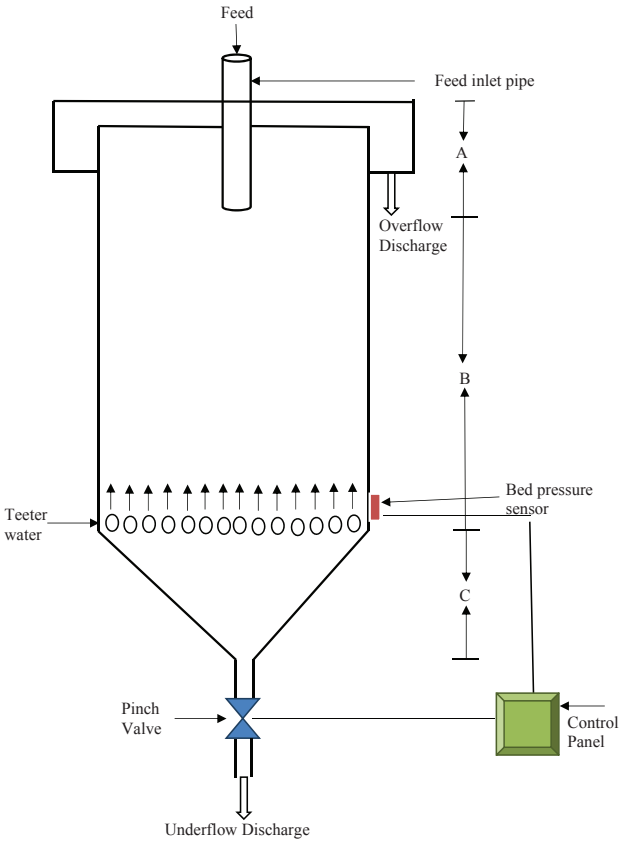

Fig.2: Schematic diagram of the set-up of Floatex Density Separator.

Processing of the as-received iron ore fines was carried out using Floatex Density Separator (Model No. LPF-0230, OUTOKUMPU). The initial stage of processing was carried out by gravity concentration as gravity separation is one of the cheapest methods of processing low-grade or waste material and no reagents are used. The FDS has a

cross-section of 230 mm×230 mm, 530 mm height of the square tank and 200 mm height of the conical section at the bottom. The feed distributor was inserted inside down to 230 mm from the top.

Experiments with Floatex density separator were carried out based on the factorial design of experiments using three variables. The variable parameters like teeter water flow rate (TW) and bed pressure (BP) are the machine parameters; however, the feed rate and percent solids on the slurry (PD) refer to the material variable. Among the four parameters mentioned, the teeter water flow rate, bed pressure and slurry pulp density were considered important variables as these have a significant effect on the yield and grade of under and overflow products of FDS. The feed rate in the form of the slurry was kept constant at 300 kg/hr throughout the study. The levels of parameters are given in Table 2. Experiments were carried out under the varied levels to optimize the condition for maximizing the yield with improved Fe-content.

Table 2: Variable parameters and levels

Parameter	Units	Levels		
Teeter water flow rate (TW)	lpm	10	14	18
Bed Pressure (BP)	kPa	5	5.5	6
Pulp density (PD)	% solid	30	40	50

The teeter water flow rate was adjusted with the support of a rotameter (flow meter) and pressure or set point was calculated and set on the PID controller. When the pressure inside the column reached the set pressure, the sensor receives the signal to open the valve actuator of the pinch valve when already settled solids could be discharged as the underflow. When the pressure becomes less than the set point the valve is actuated by the sensor and is closed. This maintains the constant pressure inside the teeter column. The fine and light particles will be discharged continuously through the overflow pipe. After completion of the feeding, the pressure is reduced to drain out the already settled solids to the underflow stream. The samples collected from both the streams i.e., underflow and overflow were analysed for Fe content.

The underflow obtained from the Floatex density separator at optimized conditions was ground to -150 μm for its better liberation. The ground product was deslimed using a 2" lab model Mozley hydrocyclone keeping the diameter of the vortex finder at 14mm and apex opening at 6.5mm. The size distribution of the ground product of hydrocyclone underflow was determined. The feed inlet pressure was varied at three levels namely10 kPa, 12kPa, and 14 kPa keeping the solid concentration at 10% to obtain the best rejection of tailing (yield and grade) to the overflow. The hydrocyclone underflow was subjected to magnetic separation for further improvement of the Fe-content of the product.

3. RESULTS AND DISCUSSION

1.1 *Characterization of as-received sample*

The characterization results of the as-received feed sample were presented in Figs. 3 and 4. The specific gravity of the different size fractions was determined using a pycnometer. The size distribution and Fe-grade in the fractions are indicated in Fig. 3, and the specific gravity of different size fractions is presented in Fig. 4. From Figure 3 it is found that around 20% and 50% of materials are of -160μm and -550μm size respectively. The -74μm fraction is 10.8% containing 31.4% Fe with 6.8% Fe distribution. The fraction +74μm is 89.2% by weight assaying 51.83% Fe and 93.2% Fe distribution. Fig. 4 shows that the coarser fractions have higher specific gravity than the finer fractions below 74μm. The reason is the presence of a higher amount of Fe content in the coarser fractions. Therefore, below 74μm was discarded from the feed by wet screening before subjecting for processing as the slimes contain more gangue minerals and also have a detrimental effect on the process efficiency**.** Desliming

of the feed material enriched the quality of the feed material from 49.81% to 51.83% and will also enhance the efficiency of the downstream processes.

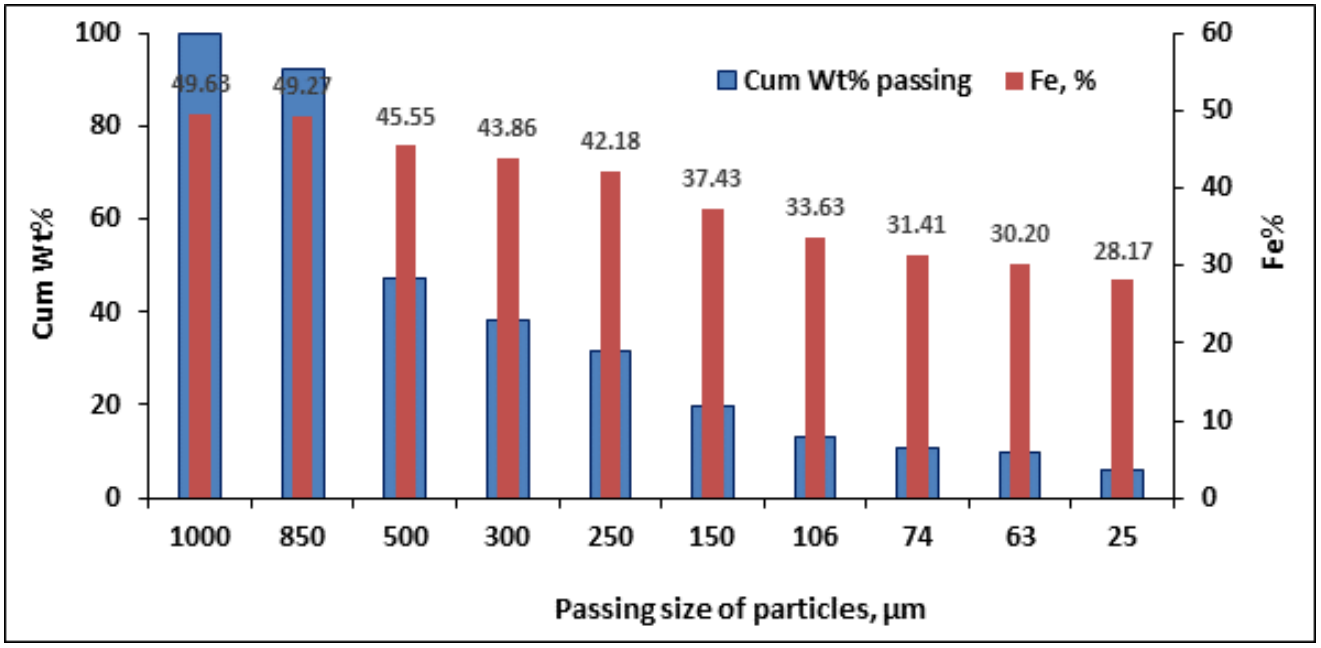

Fig 3: Particle size distribution with Fe-content of as received sample.

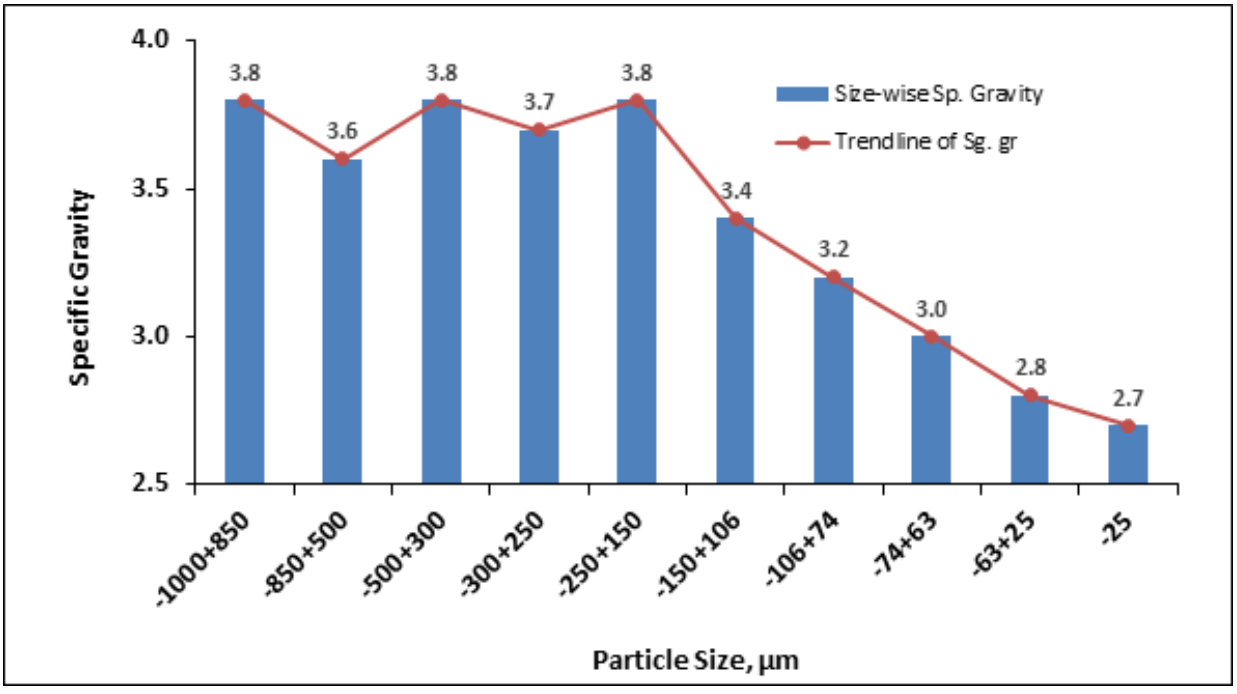

Fig.4: Size-wise density of size fractions of an as-received sample.

3.2 Floatex Density Separator

The beneficiation studies were carried out with the deslimed feed sample using a Floatex density separator based on the factorial design of experiment using three process variables at two levels (Table 2). The results obtained under the varied conditions are presented in Table 3. The effect of the process variables of FDS on the underflow and overflow products are presented in Figs. 5 and 6. The values with respect to the original feed have been indicated in the figures.

Table 3: Results of deslimed feed using Floatex Density Separator

Trial Nos.	Process Variables			Yield, %		WRO, %		Fe- Grade, %	
	Tweeter water	Bed Pressure	Pulp Density	U/F	O/F	U/F	O/F	U/F	O/F
1	10	5	30	82.7	17.3	73.8	15.4	53.5	46.4
2	18	5	30	76.3	23.7	68.1	21.1	57.4	40.4
3	10	6	30	83.2	16.8	74.2	15.0	53.9	41.4
4	18	6	30	75.3	10.7	67.2	22.0	56.7	44.7
5	10	5	50	80.2	19.8	71.5	17.7	56.0	43.1
6	18	5	50	72.2	27.8	64.4	24.8	58.2	40.0
7	10	6	50	81.6	18.4	72.8	16.4	55.1	41.2
8	18	6	50	77.7	22.3	69.3	19.9	57.0	41.1
9	14	5.5	40	81.9	18.1	73.1	16.1	55.8	43.4
10	14	5.5	40	82.7	17.3	73.8	15.4	55.8	41.3
11	14	5.5	40	83.6	16.4	74.6	14.6	55.8	41.8

3.2.1 Effect of Teeter Water flow

The role of teeter water flow is to keep the material fluidized. The effect of teeter water flow rate on the underflow yield and Fe content could be seen in Fig. 5. It was observed that within the experimental conditions, teeter water flow rate has a significant effect over the other variables. With the increase in teeter water flow rate (Trial Nos. 2,4,6 in Table 3), the yield of underflow decreases with a gradual increase in the Fe-grade (Fig. 5). Higher teeter water imposes a greater fluid drag on the particles which hinders them to settle and eventually leads more light and fine particles to the overflow resulting in less underflow yield with better Fe content [13-16]. At a higher flow rate of 18 lpm, the effect was found to be reflective and significant enrichment in Fe-content (59.6%) in the underflow was achieved with a 58.2% yield (with respect to original feed). The overflow yield is 24.8% with 40% Fe content (Fig. 6).

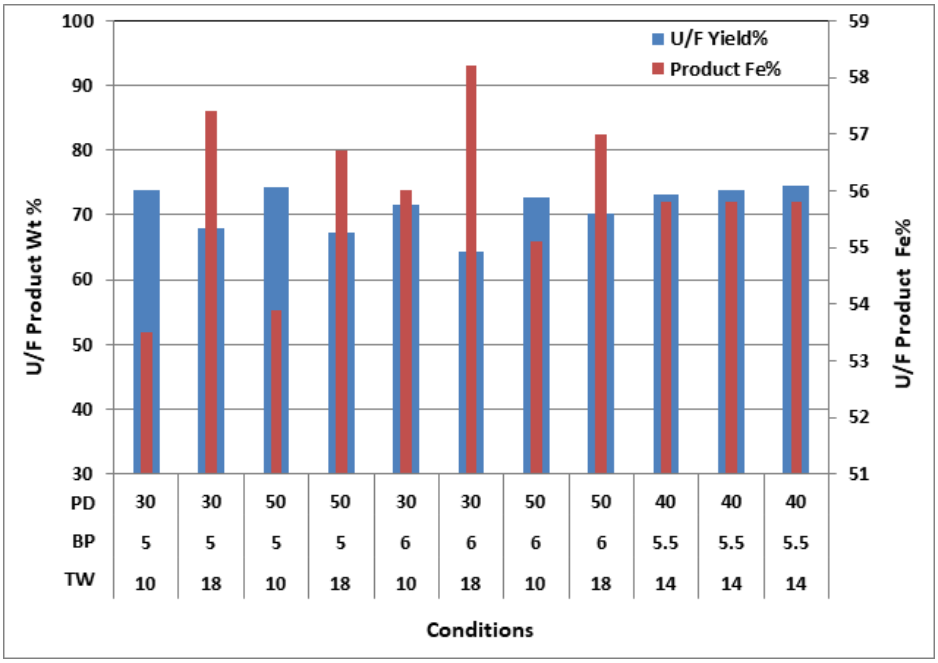

Fig. 5: Effect of variables on yield and Fe grade of Floatex underflow.

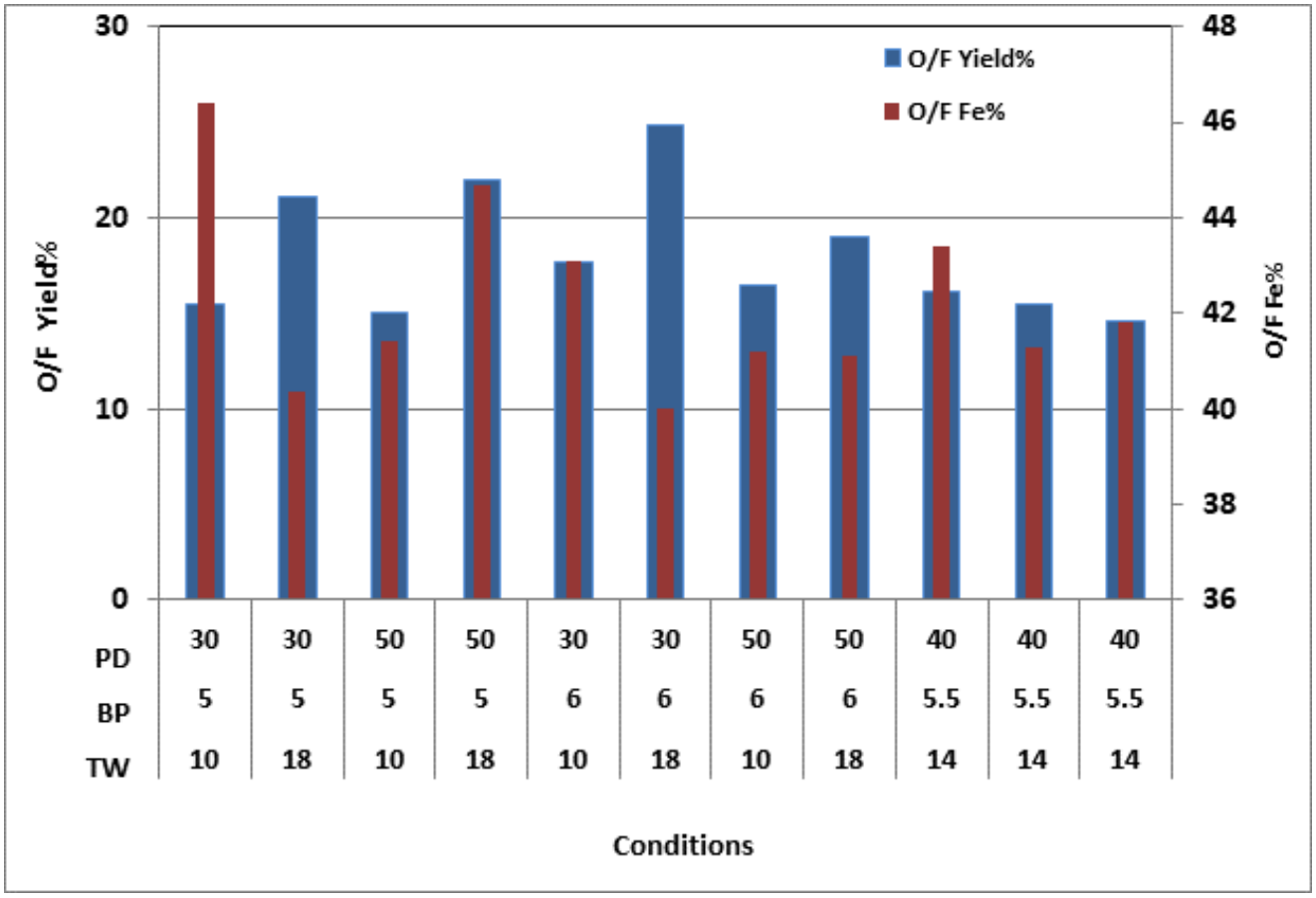

Fig. 6: Effect of variables on yield and Fe grade of Floatex overflow.

3.2.2 Effect of Bed Pressure

In the present study, the bed pressure was varied in the range of 5 to 6 kPa based on the distribution of particles in the feed. The effect of bed pressure and teeter water flow rate are inversely proportional to the responses. With increasing the bed pressure, the yield of the underflow increases with the decrease of Fe-grade (Fig. 5). Higher bed pressure results to reduce the voidage in the particle bed. Subsequently, the bed becomes more compact. As a result, increases the suspension density of the pulp and causes more rejection of the lighter particles in the overflow stream. The effect of bed pressure within the experimental variation (domain) was found to be less than the teeter water flow rate. At high bed pressure and teeter water flow rate and low pulp density (condition: BP= 6 kPa, TW=18 lpm, PD= 30%), produces an underflow yield of 64.4% with as high as 58.2% Fe-grade.

3.2.3 Effect of Pulp Density

The pulp density of the slurry defines the distribution of the feed particles. The higher the pulp density, the more is the particle-particle interaction in the slurry. It has a direct impact on the hinder settling of the particles. In the present investigation, the pulp density of the slurry was varied from 30 to 50% solid. At a higher pulp density of 50% solid, the effect of hinder settling is more and increases the effect of bed pressure, thus reducing the efficiency of the separation process. It appears from Fig. 5 and 6 that due to the more effect of teeter-water and bed pressure, the Fe-grade of the underflow product increases and yield decreases. At lower pulp density (30% solid), the rejection of lighter minerals (gangue) in the overflow is 24.8% with Fe content. Thus, a higher teeter water flow rate and low pulp density facilitate enriching the Fe content of the underflow yield.

3.3 Interaction effect of variables on responses

The results produced from the FDS based on statistical factorial design were analyzed by Design software (version 7.0) to interpret the individual and interactive effects of the process variables on the responses, like the yield of underflow and their Fe grade. The % contribution of the variables to the responses is presented in Table 4. It could be found that teeter water has more than 70% effect on the yield and Fe-content of the underflow. The regression equations generated from the ANOVA of the product (U/F) yield and Fe-grade of the yield of underflow are indicated by equations 2 and 3 respectively. The coefficients of regression equations indicate the degree of the effect. The higher the values of the coefficient, the greater the impact. It was found that teeter water (TW) and pulp density (PD) have a positive effect and the bed pressure (BP) has a negative effect on the yield of the product (U/F). The regression equation (2) shows that besides the effect of individual factors (TW, BP, PD), there is an interactive (TW-BP, TW-PD, BP-PD) effect on the product yield; however, the coefficients are not as high as the teeter water. Regression equation (3) of the Fe-grade of underflow shows that the co-efficient of the bed pressure (BP), pulp density (PD), and interaction effect of teeter water and pulp density is significant as compared to the interactive effect of the teeter water flow and bed pressure.

Table 4: Contribution of significant variables and their interaction on responses

Variables	% Conribution	Effect on responses
Response: U/F Yield		
Teeter water (TW)	74.29	Decrease
Bed pressure (BP)	2.76	Decrease
Pulp density (PD)	3.41	Increase
TW&BP	3.53	Increase
TW&PD	11.15	Increase
BP&PD	2.56	Increase
Response : U/F Fe-grade		
Teeter water (TW)	73.50	Increase
Bed pressure (BP)	7.76	Increase
Pulp density (PD)	4.59	Decrease
TW&PD	7.76	Decrease
TW&BP	1.65	Decrease

Yield of undeflow

$$= 65.35 - 5.55*TW - 1.07*BP + 1.19*PD + 1.21*TW*BP + 2.15*TW*PD + 1.03*BP*PD \quad \ldots(2)$$

Fe grade of undeflow

$$= 55.9 + 2.00*TW + 0.65*BP - 0.50*PD - 0.65*TW*PD - 0.07*TW*BP \quad \ldots.(3)$$

3.3.1 Interactive effect of teeter water and pulp density

From Table 4 and equations 2 and 3, it was found that the co-efficient of the interactive effect of pulp density and teeter water is significant on the U/F product yield and Fe-grade compared to other parameters. From Fig. 6 it is found that the yield of the overflow increases at higher teeter water flow (18 lpm) and low pulp density (30%) because the elutriating effect seems to be more at higher teeter water flow than the lower TW. As the pulp density increases the negative effect of teeter water on the yield of the underflow reduces. The combined effect of these two variables could be balanced at high pulp density and teeter water flow, and low bed pressure.

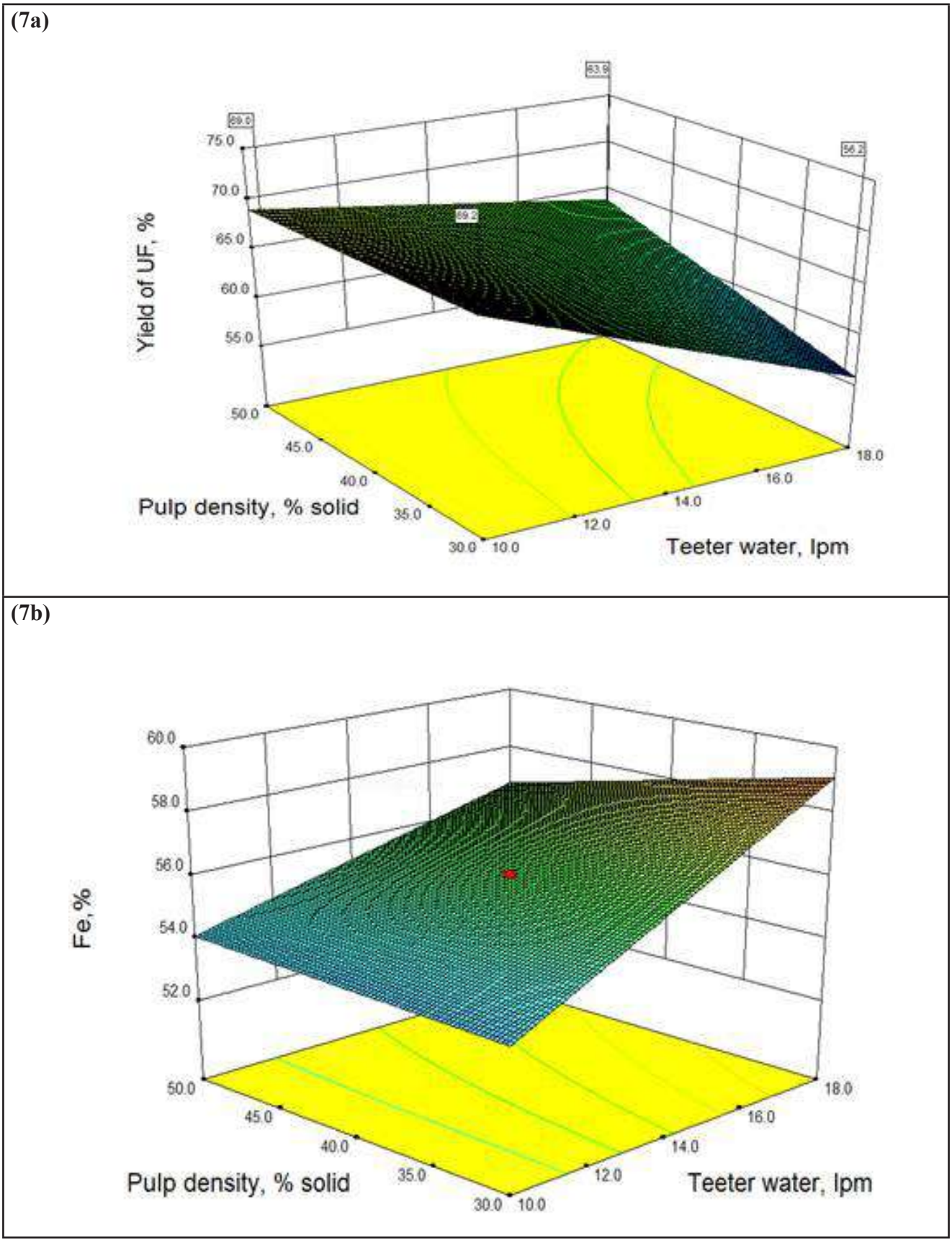

Fig. 7: Interaction effect of teeter water and pulp density on (a) underflow of FDS and (b) Fe-grade.

3.3.2 Interaction effect of teeter water and bed pressure

The interactive effect of teeter water flow rate and bed pressure is shown in Fig. 8. The role of teeter water flow rate and bed pressure on the suspension density is inversely proportional to the bed voidage. The increased teeter water flow dilates the bed and increases the viodage, whereas the bed pressure reduces the voidage and makes the bed more compact [15-16]. Thus, increased bed pressure increases the density of the medium produced during the separation. Between the two opposite effects, water flow rate has been found to be more dominating as shown in Table 4. With increasing the teeter water flow rate and bed pressure, the yield of the overflow increases. As a result, the Fe- content of the U/F increases with reduced mass. Therefore, the separation performance of FDS depend significantly on the selection of the operating conditions.

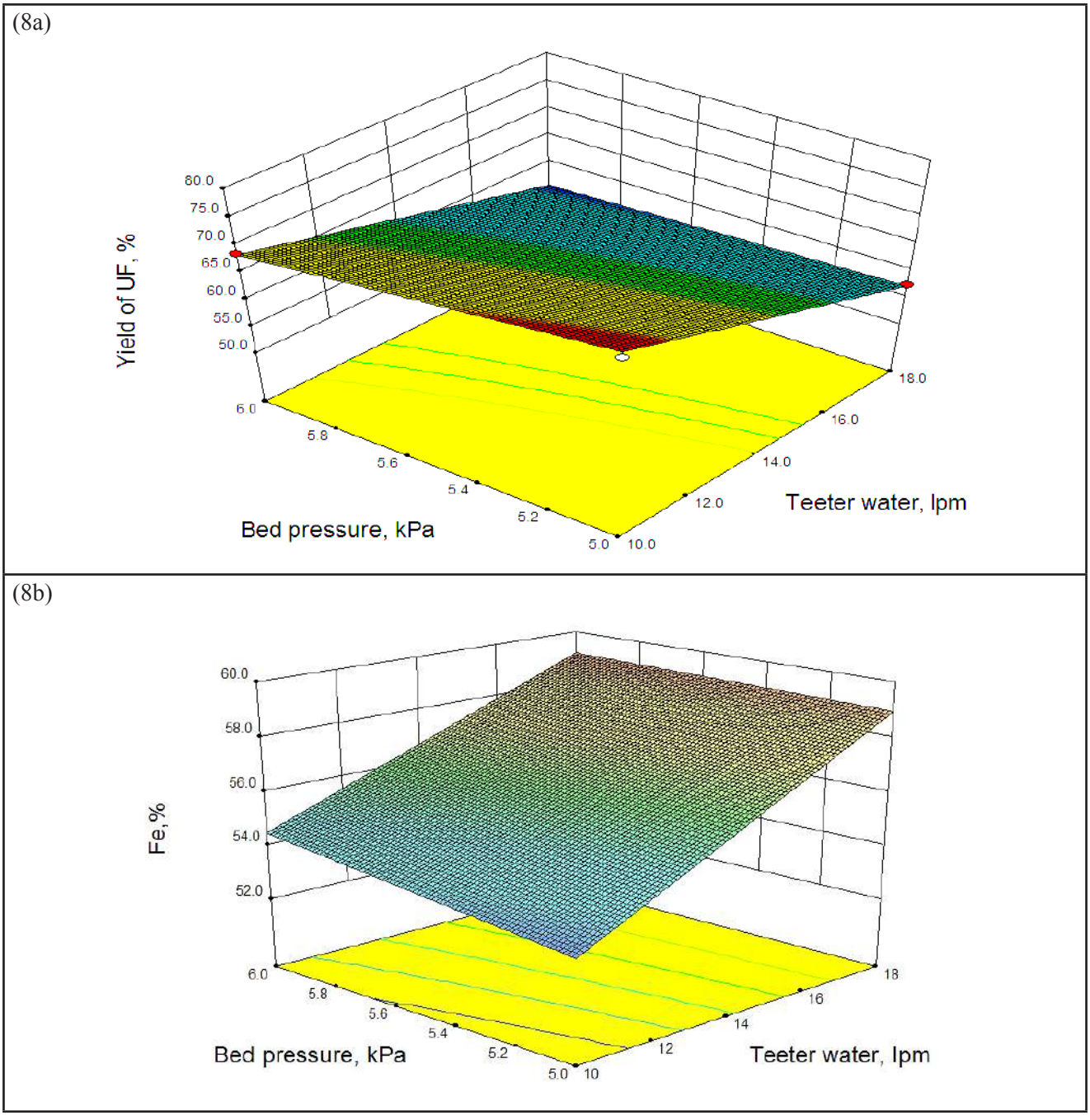

Fig.8: Interaction effect of teeter water and bed pressure on yield of (a) underflow of FDS and (b) Fe-grade of products.

3.3.3 Effect of Bed Pressure and Pulp Density

The interaction effect of bed pressure and pulp density on underflow product is shown in Fig. 9. At low bed pressure, the autogenous media could not develop and the FDS behaves like an elutriator. The fine particles are carried out of the fluidized bed by the upward flow of the fluid. The high bed pressure increases the density of the autogenous heavy media developed inside the chamber. With the increase of the pulp density increases the distribution of feed particles in the slurry; thereby increases the effect of hinder settling. With increasing the bed pressure from 5 to 6 kPa, and pulp density of 30 to 50 % solids, yield to underflow increases. The effect was found to be more dominant with the pulp density because the increase in the suspension density decreases the void density, which in turn compresses the bed. Therefore, the effective separation was found at the level of 30% PD, BP of 6kPa and teeter water flow rate of 18 lpm.

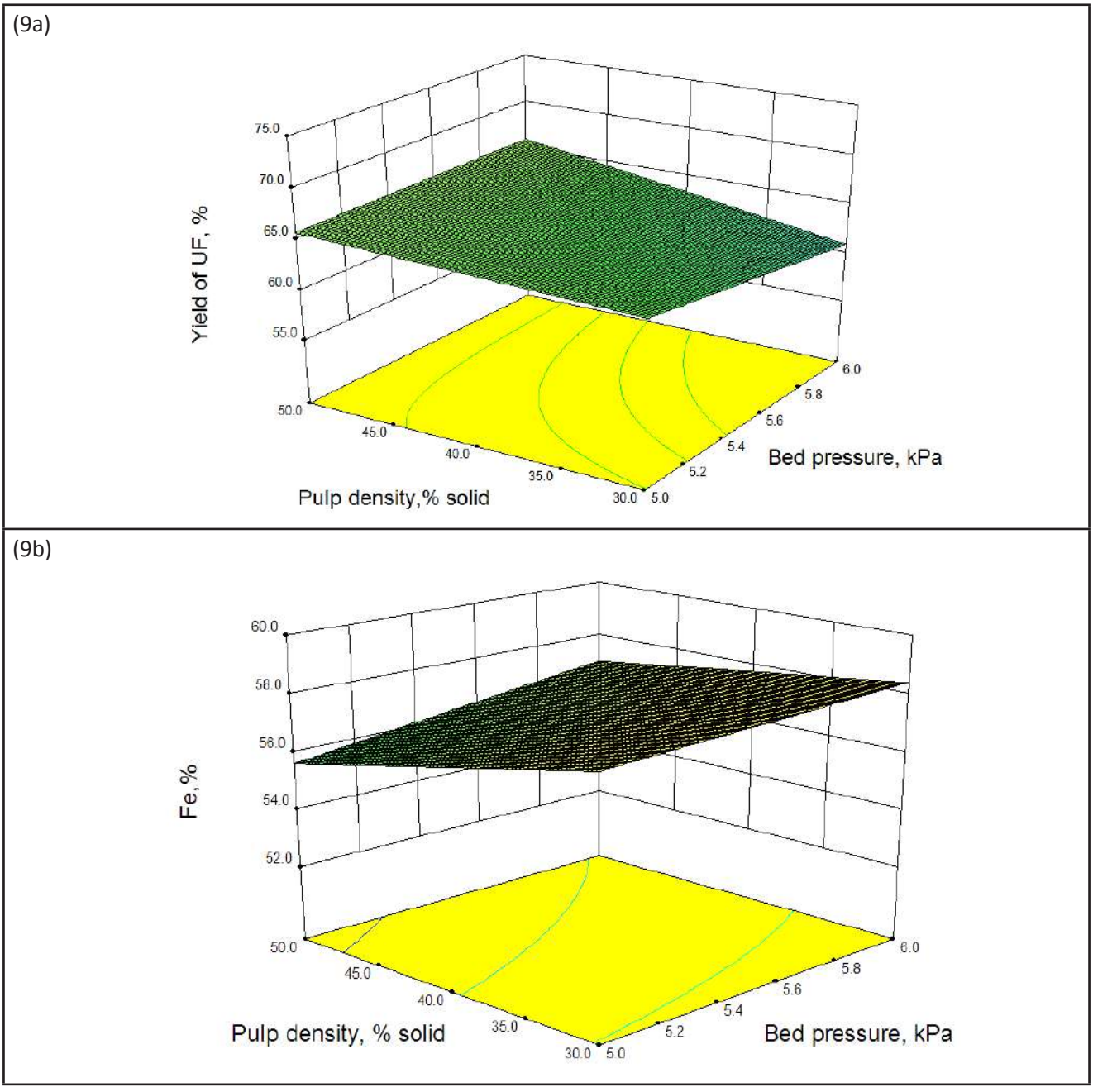

Fig.9: Interaction effect of bed pressure and pulp density on (a) underflow of FDS and (b) Fe-grade.

3.4 Processing of underflow of Floatex Density Separator

As the major iron-bearing mineral in the dumped sample was hematite, having a minor amount of martite, there is a possibility for further improvement of the quality of the product to make it useable for pellet feed. The underflow obtained from FDS was ground to -150µm. It was found from the particle size distribution (PSD) of the groundmass of underflow that the weight percent of 106µm fraction is about 54.6% and -10µm fraction is about 17.4% out of 64.7% product weight. The ultrafine particles are detrimental to the separation process, and thus, reduce the efficiency. It was discarded using hydrocyclone before subjecting to the magnetic separation for Fe enrichment. The result of desliming of -150µm ground product of FDS underflow using hydrocyclone is given in Table 5.

Table 5: Results of desliming at different pressures

Conditions	Product	Wt%	WRO	% Fe	Fe Recovery, %
10 psi VF= 14mm, Apex= 6.5mm	U/F	85.8	55.3	60.29	65.6
	O/F	14.2	9.1	44.9	8.1
12 psi VF= 14mm, Apex= 6.5mm	U/F	89.9	57.9	59.45	67.9
	O/F	10.1	6.5	45.2	5.8
14psi, VF= 14mm, Apex= 6.5mm	U/F	93.4	60.1	58.96	70.0
	O/F	6.6	4.3	44.46	3.7

The diameter of the vortex finder and apex opening was kept constant based on the earlier experience and from reported literature [17]. The effect of feed inlet pressure on the yield of the underflow and grade is shown in Fig. 10. From these figures it can be seen that yield to underflow is increasing with pressure and the grade of underflow is decreasing. This is due to the increase of the centrifugal forces generated by spin which forces the coarser particles to move towards the wall of the cyclone. The 10psi feed pressure was found to be suitable to remove the ultrafines in overflow with 44.9% Fe content as indicated in Table 5. The yield of underflow is 55.3% with respect to the original feed, with an assay value of 60.29% Fe and Fe recovery of 65.6%. This de-slimed material was used as feed for the wet high intensity magnetic separation (WHIMS).

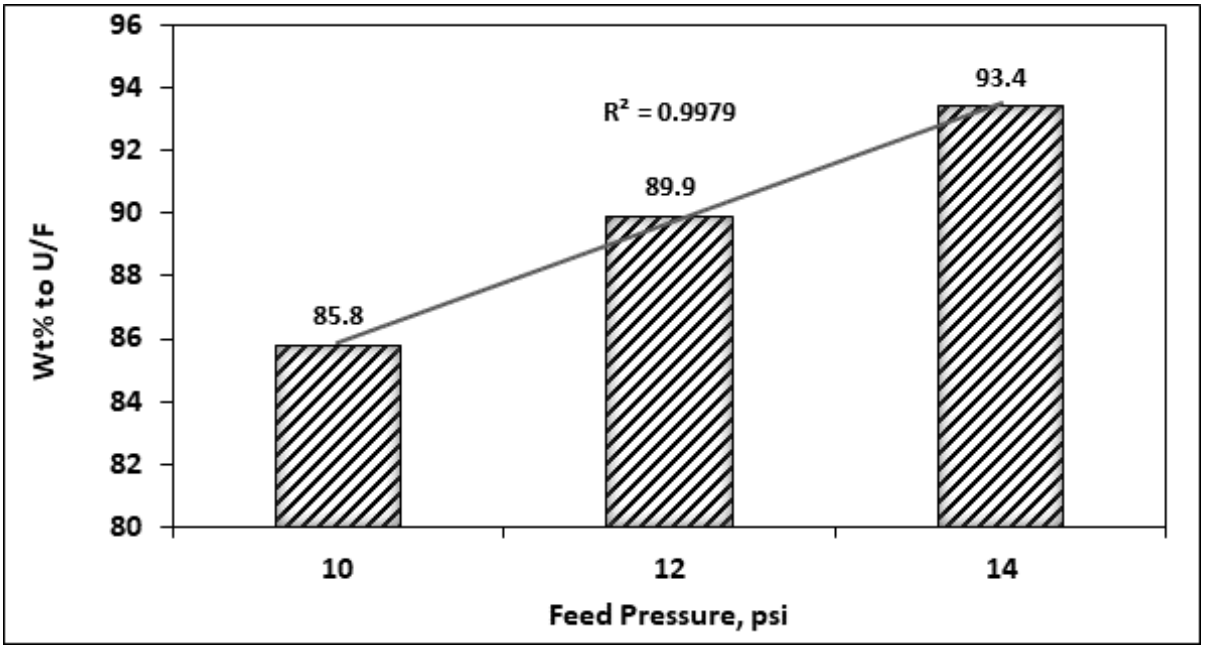

Fig.10: Effect of feed inlet pressure on underflow wt%.

3.4.1 Processing of FDS-Underflow of by WHIMS

The underflow obtained from the hydrocycloning of the ground mass of FDS-U/F having grade 60.29% Fe was fed to the high intensity magnetic separation (WHIMS). While conducting the experiments, the pulp density of 10% solid and the matrix gap of 0.5mm were kept constant. The current intensity varied from 2A to 4A. As the magnetic intensity is directly proportional to the current intensity, it changes the magnetic field intensity. The effect of magnetic intensity on the yield of concentrate and grade is shown in Fig. 11. It is observed that the yield of magnetic product was less at low magnetic field intensity as the highly susceptible (ferromagnetic) materials having high Fe-content are attracted. At high magnetic intensity, the yield of concentrate is high with a lower grade than that of concentrate at lower magnetic intensity. The condition with 3amp current (1.0 T magnetic intensity) seems to be optimum condition where the product yield is reasonable with an optimum grade of concentrate. The product weight% is 44.5% with 62.1% Fe content, and 37.8% yield with 63.4% Fe content.

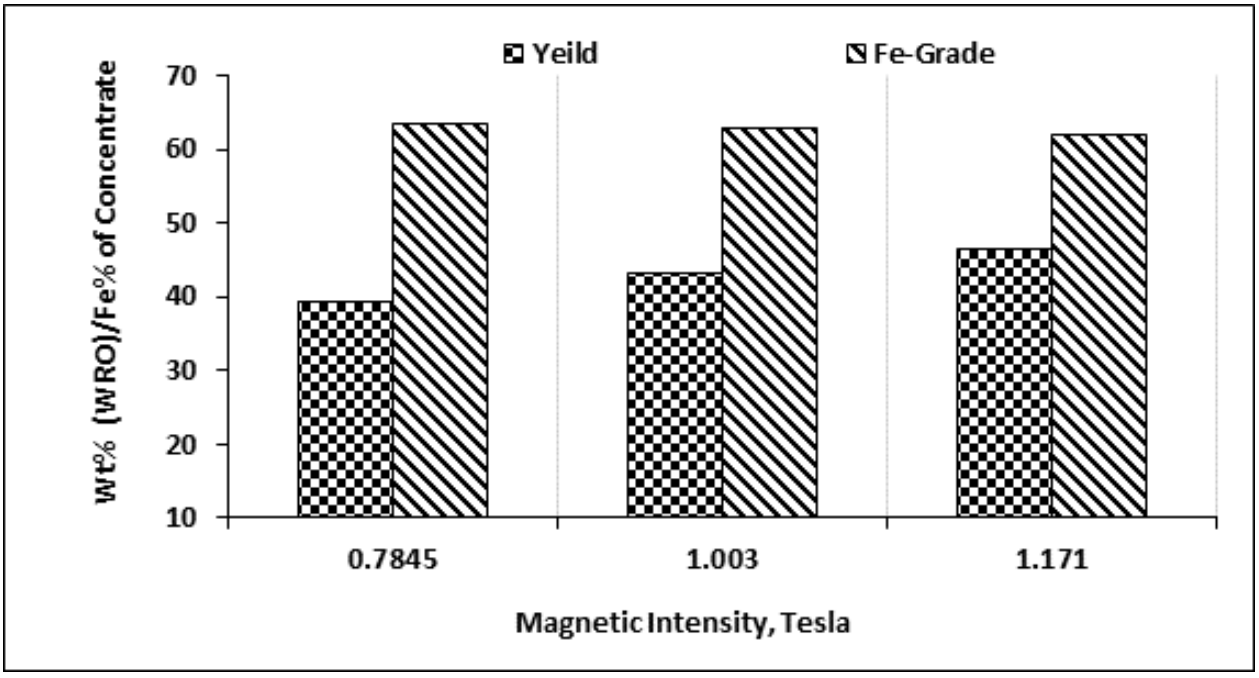

Fig.11: Effect of Magnetic intensity on concentrate yield and grade.

4. CONCLUSIONS

The present investigation highlights the response of the low-grade iron ore dumps having 49.62% Fe, 6.96% SiO_2, 9.94% Al_2O_3 and 7.65% LOI using a floatex density separator as a gravity concentrator at the initial stage of processing, and its metallurgical performance has been studied using a statistical design of experiments. In the sample, presence of main iron-bearing mineral phases like hematite, goethite, and a small amount of martite favours the separation efficiency of FDS. It has been found that the teeter water flow is more prevailing than the other variables like pulp density and bed pressure in the present investigation. The high teeter water flow keeps the bed suspension and moves the lighter density particles to the overflow steam as a reject. The high bed pressure of the slurry may not be effective for separation.

Because of the presence of some interlocked particles in the sample, Fe-content of the FDS underflow could be improved up to 58.2% with a yield of 64.4%. Further size reduction of the underflow product to 150μm improves the liberation of gangue minerals and subsequent hydrocycloning produces a product with an assay of 60.3% Fe with a mass of 55.3%. Further enrichment of Fe-grade by magnetic separation produces pellet grade feed. Thus, processing of dumped low grade iron ore towards the production of value-added product has an enormous impact on the environment and conservation of the resources.

ACKNOWLEDGMENTS

The authors would like to extend their sincere thanks to the Ministry of Steel for funding the research work (GAP 0224).

DECLARATION OF COMPETING INTEREST

The authors declare that they have no known competing financial interests or personal relationships that could have appeared to influence the work reported in this research article.

5. REFERENCES

1. Tripathy, S.K.; Mallick, M.K., Singh, V., Murthy, Y.R., Preliminary studies on teeter bed separator for separation of manganese fines. Powder Technol, 239, 284–289, 2013.
2. Carpenter, J.L.; Iveson, S.M.; Galvin, K.P., Ultrafine desliming using REFLUX (TM) classifier subjected to centrifugal G forces. Miner. Eng., 134, 372–380, 2019.
3. Ozcan, Ö.; Ergun, S.L., Performance of teetered bed separator for non-coal applications. Sep. Sci. Technol. 52, 1486–1495, 2017.
4. C. Raghukumar, Sunil Kumar Tripathy, S. Mohana, Beneficiation of Indian High Alumina Iron Ore Fines – A Case Study, International Journal of Mining Engineering and Mineral Processing, 1(2): 94-100, 2012.
5. Raghu Kumar, Sunil Tripathy and D.S. Rao, Characterisation and pre-concentration of chromite values from plant tailings using Floatex Density Separator, Journal of Minerals & Materials Characterization & Engineering, Vol. 8, No.5, 367-378, 2009.
6. T. Umadevi, Abhishek Kumar, A Umashanker, Rameshwar Sah & K. Marutiram (2021) Performance evaluation of a laboratory floatex density separator and its comparison with a spiral concentrator, Mineral Processing and Extractive Metallurgy, 130:2, 118-125, DOI: 10.1080/25726641, 2019.
7. Galvin, K.P., Pratten, S.J., Nicol, S.K., Dense medium separation using teetered bed separator. Minerals Engineering, 12 (9), 1069–1081, 1999.
8. Floatex Density Separator by Floatex, web link: http://www.floatex.co.uk/wp-content/uploads/2019/08/Floatex-Density-Separator.pdf**.**
9. Raghu Kumar, C., Singh, R.R., Venugopalan, O.K., Murry, V.S. and Kumar, S.S., Effect of teetering pulp density in Floatex Density separator- A Case Study' Proceedings of the International Seminar on Mineral Processing Technology - Chennai, India, 564 – 567, 2006.
10. Chandrakala K., G. K., Rao, S. Mohan and Rao, N. D., Predicting the chromite mineral upgradation in Floatex Density separator using hindered settling models' ISIJ International, Vol. 46, No. 7, 966–973, 2006.
11. Murthy, N., Basavaraj, K., Assessing the performance of a Floatex Density Separator for the recovery of Iron from low-grade Australian iron ore fines – A Case Study' XXVI International Mineral Processing Congress (IMPC), 03612-03621, 2012.
12. Xing, Y.; Gui, X.;Wang, Y.; Cao, Y.; Zhang, Y., Optimization of teetered bed separator using pulsed water. Int. J. Coal Prep. Util. 36, 283–292, 2015.
13. Zhu, X., Liu, J., Cao, Chao, Dong, Y. and Tao, W., Numerical Studies on Teeter Bed Separator for Particle Separation, Energies, 2020, 13, 2025; doi:10.3390/en13082025.
14. Ghatage, S.V., Khan, S.M.; Peng, Z., Doroodchi, E.; Moghtaderi, B., Padhiyar, N., Joshi, J.B., Evans, G.M., Mitra, S, Settling/rising of a foreign particle in solid-liquid fluidized beds: Application of dynamic mesh technique. Chem. Eng. Sci. 170, 139–153, 2017.
15. Xia, Y.K., CFD Simulation of fine particle gravity separation in hindered-settling bed separators. Chem. Prod. Process. Model, 2, 1–21, 2007.
16. Bharath N, Swapnil Urankar, Venkatesh, L K, Ramkumar, Aditya, Dua, R., Effect of particle drag on performance of a Conical Base Classifier' International Journal on Theoretical and Applied Research in Mechanical Engineering, Vol 3, Issue-3, 2014.
17. Ghatage, S.V., Sathe, M.J., Doroodchi, E., Joshi, J.B. and Evans, G.M, Effect of turbulence on particle and bubble slip velocity. Chem. Eng. Sci., 100, 120–136, 2013.
18. Yanxia Xu, Xingfu Song, Ze Sun, Bo Tang, Ping Li, Jianguo Yu, Numerical investigation of the effect of the ratio of the vortex-finder diameter to the spigot diameter on the steady-stat of the air core in a hydrocyclone, Industrial & Engineering Chemistry Research, 52(15):5470–5478, 2013.

Preparation of Manuscripts

1. Manuscripts should be sent in MS Word and pdf format.
2. Text should be 12 pt Times New Roman, double-spaced, left justified, A4 sized paper with wide margin.
3. All pages should be numbered consecutively, beginning with page 1, the title page.
4. Tables and figures should be numbered serially. Figures should have legends if applicable.
5. Tables and figures will be placed near their first mention in the text; all tables and figures must be referred to in the manuscript.
6. The following information must be included:

- Title of the article;
- Name(s) and initial(s) of author(s)
- Affiliation(s) of author(s);
- Name, address, telephone, mobile number and e-mail address of the corresponding author.
- **Abstract:** Each article should include a brief abstract of 250 words, thatshould highlight the objectives, methods, results, and conclusions of the paper.
- **Keywords:** To identify the subjects under which the article may be indexed, 6-10 key words should be provided.
- **References:** In the text, references to the literature should be presented within square bracket indicating the reference number [1]
- **Paper:**

  [1] J. Singh, A. Kumar: Investigation of structural, morphological and electrochemical properties of mesoporous La_2CuCoO_6 rods fabricated by facile hydrothermal route. Int. J. Miner. Metall. Mater. 27: 987–995, 2020

- **Book:**

  [2] J.D. Verhoeven: Fundamentals of physical metallurgy, 1st Edition, New York: Wiley, New York, pp. 55-61, 1975

- **Online document**

  [3] Cory Mitchell: Fractal Indicator Definition and Applications. Technical analysis basic education. Available via https://www.investopedia.com/terms/f/fractal.asp, Retrieved 3 August 2020

- **Illustrations :** These include photographs, drawings and line art includes graphs, flowcharts, diagrams etcwhich can be reproduced without losing any clarity. Figure legends or captions should follow the order in which they appear in the manuscript, be numbered with Arabic numerals and should not contain a text repeated. The preferred file formats for images and line art are TIF/TIFF and JPG. For good image quality, scanned black & white photographs should be provided as 300 ppi TIFF files and line art should be provided as 600 ppi TIFF files.
- **Color Figures :** The authors should accept the obligation of bearing the expenses of colour images in the printed version of the journal while no charge is required for their appearance in the electronic version of the journal. Colour illustrations should be provided as scanned TIFF files at a minimum of 300 ppi with a 24-bit colour depth.
- **Mathematical Equations :** Mathematical equations, suitably numbered, should be inserted in the text through "Equation editor" of MS word as per the example

$$P(e) = \frac{1}{2}\left[1 - erf\left(\frac{K}{2\sqrt{2}}\right)\right]$$

- Symbols, Abbreviations, Units, etc.: It is mandatory to define the symbols and acronyms at first mention within the text and also in titles and abstracts. The authors are requested to follow internationally accepted rules for nomenclature, abbreviations, symbols and units.
- **Computer Code:** Pseudo algorithms, as presented below, with appropriate reference should be submitted.
  - **Title** : To compute power spectral density and corresponding frequency

    Input : Time domain data X(t)

    Output : P

    - Read the signal X(t)
    - Crop the signal and get the length N
    - Supply sampling frequency, f_s
    - Do fast Fourier transformation of the signal

      Xk = fft(X(1:N), f_s);
    - Compute power spectral density and corresponding frequency by

      P = Xk.*conj(Xk) / N;

      f = fs*(1:f_s)/N;